ORIGINAL PAPER

Landslide susceptibility of volcanic landforms in the Río El Estado watershed, Pico de Orizaba volcano, Mexico

**Gabriel Legorreta Paulín · Marcus I. Bursik ·
José Juan Zamorano Orózco · José Ernesto Figueroa García**

Abstract The combination of high-quality landslide inventories and geomorphic attributes that can be derived and analyzed by geographic information systems can provide powerful and straightforward input into mapping landscape-wide landslide susceptibility. A methodology for generating landslide susceptibility maps can assist land managers in reducing risk to populations and economic land use from landslide hazards, particularly in areas prone to landslide disasters, such as tropical mountain ranges. Pico de Orizaba is the highest stratovolcano in Mexico, and throughout its geologic history, it has had large landslides triggered by flank collapse as well as small landslides triggered by high seasonal rainfall on terrains covered by poorly consolidated materials. The present work analyzes the distribution of small landslides embedded in volcanic landforms to characterize slope instability. The Río El Estado watershed on the southwestern flank of Pico de Orizaba volcano has been selected as a study area. In the area, landforms are ascertained through aerial photographs, field investigations, and an adaptation of the Landslide Hazard Zonation Protocol of the Washington State Department of Natural Resources, Forest Practices Division in a GIS-based technology. For each landform, a semi-quantitative overall susceptibility rating is derived by using the landslide area rate and the landslide frequency rate. This analysis divides the watershed into seven mass-wasting landforms that are assigned slope stability susceptibility ratings from low to very high. The overall susceptibility rating for this watershed is very high. The technique and its implementation are presented and discussed.

G. Legorreta Paulín (✉)
Laboratorio de Análisis Geo-espacial, Instituto de Geografía, Universidad Nacional Autónoma de México, Circuito Exterior, Ciudad Universitaria, 04510 Coyoacán, México, D.F., Mexico
e-mail: legorretag@hotmail.com

M. I. Bursik
Department of Geology, University at Buffalo, SUNY, Buffalo, NY 14260, USA

J. J. Zamorano Orózco · J. E. Figueroa García
Departamento de Geografía Física, Instituto de Geografía, Universidad Nacional Autónoma de México, Circuito Exterior, Ciudad Universitaria, Coyoacán 04510, México, D.F., Mexico

1 Introduction

In Mexico, an active volcanic chain extends for 1,000 km in an approximate east–west direction from the Pacific Ocean to the Gulf of Mexico. This geologic-geomorphic structure, the Trans-Mexican Volcanic Belt (TMVB) physiographic province (Fig. 1), embraces many dormant and active stratovolcanoes and monogenetic fields (Verma 1987; Centro Nacional de Prevención de Desastres 2001). The area is prone to landslides because of conditions such as volcanic activity, earthquakes, high rainfall during the wet season, poorly consolidated ash fall and other pyroclastic deposits, a high degree of weathering, and steep slopes.

In the eastern part of the TMVB physiographic province, Pico de Orizaba volcano is the highest dormant stratovolcano (5,675 m a.s.l.). The physiographic conditions predispose it to episodic evacuation of debris flows by both deep and shallow mass movement followed by slow refilling with colluvium. The risk associated with debris flow is increased by the
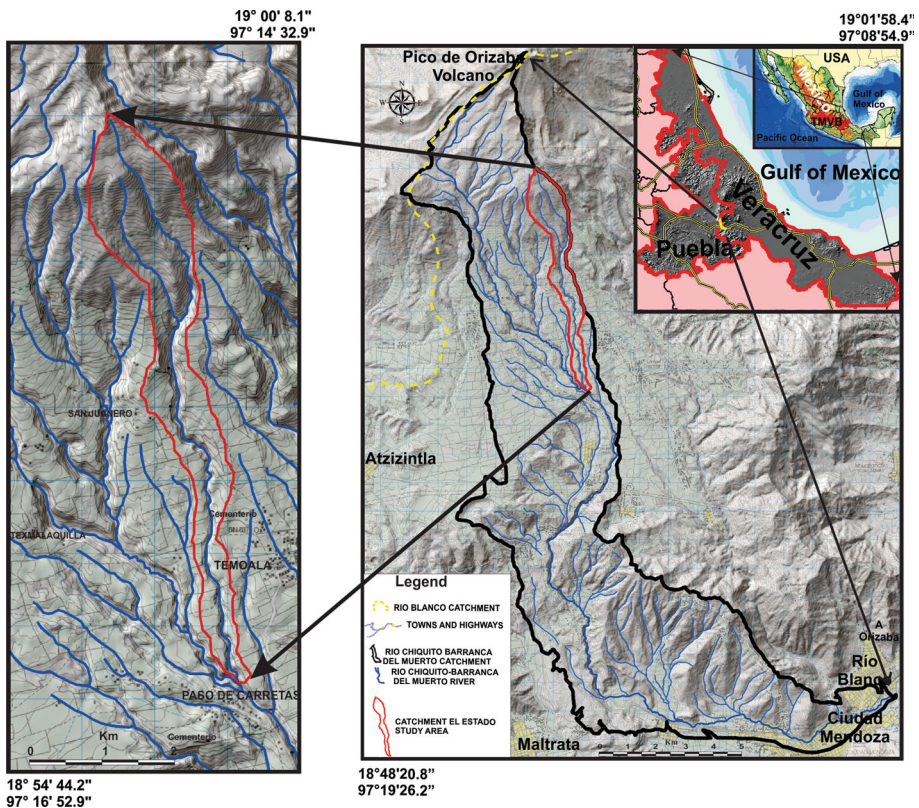

Fig. 1 Location of the study area in the Trans-Mexican Volcanic Belt (TMVB)

lack of significant volcanic activity at Pico de Orizaba over the past 147 years (De la Cruz-Reyna and Carrasco-Núñez 2002), which has led to increased human settlement and economic activity along its flanks. This creates a hazardous situation for 360,000 people living on the southern flank, where landslides along the stream system threaten towns such as Córdova, Orizaba, Río Blanco, Nogales, and Ciudad Mendoza (Instituto Nacional de Estadística y Geografía 2010). For example, in 2003, rainfalls triggered landslides on the up-stream southern flank. The landslide sediments increased the destructive power of a debris flow that caused loss of life and property at the town of Balastrera (a settlement at the base of the volcano). The Mexican oil company (PEMEX), of which multiple conduits were destroyed in the debris flow event, constructed retention walls and gabions along the lower valley of the Río Chiquito-Barranca del Muerto to protect the conduits. However, no landslide inventory or landslide susceptibility zonation was undertaken for the middle and upper portion of the watershed; and in 2011, a new landslide event destroyed the retention walls and gabions.

At Pico de Orizaba, efforts to assess volcanic susceptibility and slope stability have used GIS and remote sensing (Hubbard 2001; Sheridan et al. 2001; Hubbard et al. 2007; Legorreta et al. 2014) to make predictive maps somewhat more helpful and suitable for engineers, policy-makers, and developers who seek to carry out landslide susceptibility mitigation. However, the landslide susceptibility has been difficult to evaluate owing to large spatial and temporal variability as well as a lack of landslide inventory maps.

In light of the above, the El Estado watershed on the southwestern flank of Pico de Orizaba volcano has been selected as a case study area to provide standardized methods for conducting semi-quantitative overall susceptibility ratings for each volcanic landform by using the landslide area rate and the landslide frequency rate from the Landslide Hazard Zonation Protocol of the Washington State Department of Natural Resources (WA DNR), Forest Practices Division (2006). In the study area, a preexisting inventory of 107 landslides covering 0.088 km^2 (Legorreta et al. 2014) is used to assess and describe landslide distribution. The volcanic landscape is classified into landform units based on morphometric parameters, aerial photographs, field investigations, GIS thematic layers (such as elevation, slope, hill shade, aspect map, and geological map), and expert knowledge (Dikau et al. 1995; Washington State Department of Natural Resources, DNR, Forest Practices Division 2006; Evans 2012). This analysis divides the watershed into seven volcanic mass-wasting landforms that are assigned slope stability susceptibility ratings from low to very high. The susceptibility rating is calculated for each volcanic landform by using the landslide area rate (LAR) and the landslide frequency rate (LFR). The technique and its implementation are presented and discussed as well as the implications for the landslide susceptibility associated with the El Estado watershed at Pico de Orizaba volcano.

2 Background

Many geographic information system (GIS)-based applications have been used throughout the world to represent and assess landslide susceptibility and landslide hazard; each uses a heuristic, statistical, or deterministic approach at a local or regional scale, and each has advantages and limitations (Anbalagan and Bhawani 1996; Van Westen et al. 1997; Hammond et al. 1992; Montgomery and Dietrich 1994; Pack et al. 1998; Parise 2001; Zhou et al. 2003; Lee et al. 2004; Xie et al. 2006; Qiu et al. 2006). During a landslide susceptibility modeling and Landslide Hazard Zonation analysis, one of the most important geomorphological characteristics to be considered is the presence or absence of landslides.

To accomplish the task of modeling, the distribution and abundance of landslides are expressed through the use of landslide inventory maps and by the subdivision of a land area into landforms (Iwahashi et al. 2001; Washington State Department of Natural Resources, DNR, Forest Practices Division 2006; Hervás and Bobrowsky 2009; Blahut et al. 2010; Evans 2012; Jasiewicz and Stepinski 2013). The interpretation and analysis of the relationships among landforms and gravitational processes are indispensable for landslide susceptibility and hazard zonation projects, not only to establish the extent of landslide hazard in an area, but also to highlight advantages and limitations of the landslide susceptibility and hazard maps (Stallins 2006; Dietrich et al. 2003; Legorreta and Bursik 2009). For landslide analysis, landforms have been defined as a basic geoform or geomorphic unit in an area, characterized by a unique combination of geometry, materials, process, and history (Evans 2012; Zinck 2013). Definition and delineation of landforms for landslide susceptibility and hazard zonation have been conducted worldwide through various approaches dictated by the scale of the analysis, the requirements of the users, and time and funding availability (Washington State Department of Natural Resources, DNR, Forest Practices Division 2006; Corominas and Moya 2008; Evans 2012). These approaches include visual identification with expert knowledge and empirical evidence as well as automatic mapping using geomorphological parameters, first and second derivates from digital elevation models, filter techniques, and statistical analysis (Pennock et al. 1987; Pike and Dikau 1995; Washington State Department of Natural Resources, DNR, Forest Practices Division 2006; Iwahashi and Pike 2007; Minar and Evans 2008; Evans 2012; Jasiewicz and Stepinski 2013). For example, since the 1990s, the Washington State Department of Natural Resources, Forest Practices Division, USA, has had a Landslide Hazard Zonation (LHZ) project whose goal is to create a slope stability screening and management tool by identifying landforms with landslide hazard in order to better describe and map all potentially unstable slopes where forest practices might occur. Landforms are linked (via the landslide inventory) to a level of hazard and sensitivity to land management (Vaugeois 2003; Legorreta et al. 2008). In Mexico, local or regional analysis and mapping of landslide phenomena have been performed (e.g., Bocco 1983; Tapia-Varela and López-Blanco 2002; Bolongaro-Crevenna et al. 2005; Capra and Lugo-Hubp 2006 Pérez-Gutiérrez 2007; Secretaría de Protección Civil 2010). These studies have analyzed landslide types, triggering mechanisms, and landslide hazard reconnaissance. In the last decade, there has been significant improvement in the procedures for data capture, data analysis, and representation through the use of GIS and remote sensing. For example, in 2010, the Secretariat of Civil Protection of Veracruz State in collaboration with other federal and state government agencies published an atlas of geological and hydro-meteorological hazards at the state level, and in 2011, the Federal Government through the Secretariat of Social Development published an atlas of natural hazards at the municipal level based on the use of GIS (Secretaría de Protección Civil 2010; SEDESOL 2011). For Pico de Orizaba, the volcanic hazard has been assessed by computer simulations of lahars with GIS and remote sensing (Hubbard 2001; Sheridan et al. 2001; Hubbard et al. 2007). In the present study area, a multi-temporal inventory map and a landslide susceptibility map are created by means of multiple logistic regression (MLR). The model is implemented with the GIS platform LOGISNET (Legorreta et al. 2014).

Despite these efforts, there is no standardized procedure to prepare landslide susceptibility or hazard maps. Also there is a lack of systematic comparison of landslide models that could outline advantages and limitations of the methods. This is due to the difficulties of assessing a model in natural conditions with different cartographic scales, DEM resolutions, and sampling strategies (Haneberg 2005; Chinnayakanahalli et al. 2003; Borga

et al. 2002; Morrissey et al. 2001; Guzzetti et al. 1999). In order to standardize such procedures, it is necessary to calibrate the mapping of landslides and landforms in a well-known and manageable pilot study area.

3 Study area

The Río El Estado watershed is at 18°55′23″–18°59′36″ N and 97°16′17″–97°14′56″ W, on the southwestern flank of Pico de Orizaba volcano within Puebla and Veracruz states, Mexico (Fig. 1). From the administrative point of view, 51 % of the area belongs to the municipality of Atzitzintla, Puebla, and 36.1 and 7.7 % to La Perla and Mariano Escobedo municipalities of Veracruz, respectively. The study area covers 5.2 km^2: 23.7 % of the land is designated for forest use and 76.3 % for agriculture and other uses. The basin is elongated with a length of 13 km and an average width of 0.72 km. The average slope on the river bed is $\sim$30.6 % ($\sim$17°), although along the watershed some places (valleys of relatively flat plains) have slopes of 8.7 % (5°), whereas in others (valley walls and steep hillslopes), the values exceed 100 % (>45°). The study area is a large piedmont characterized by hilly and steep terrain with elevations from 2,677 to 4,248 m a.s.l. and composed of pyroclastic materials, lava flows, landslide deposits, and alluvial sediment. El Estado river is a sub-basin of Río Chiquito-Barranca del Muerto watershed—a tributary of the Río Blanco—which flows into the Gulf of Mexico. The stream system of El Estado erodes andesitic and dacitic Tertiary and Quaternary lavas, pyroclastic flows, and fall deposits. Along the stream system, shallow landslides predominate on steep hills capped by ash and pyroclastic deposits. The steep hills typically experience episodic evacuation of debris by shallow mass movement followed by slow refilling with colluvium (Fig. 2c). Where the stream erodes lava flows and lahar deposits, rockfalls have occurred (Fig. 2b). Active and dormant deep-seated landslides are found in ash and pyroclastic deposits (Fig. 2d).

4 Methods

The method presented here is modified from the original used in the Washington Forest Practices Protocol to address landslide hazards (Washington State Department of Natural Resources, DNR, Forest Practices Division 2006), but it has been adapted to meet specific needs for mapping landslide susceptibility in volcanic terrains. The method encompasses all the steps followed by WA DNR to generate a hazard map, but it does not use the WA DNR SLPSTAB susceptibility model (Bilderback and Brunengo 2007; Shaw and Johnson 1995) because landslide processes in volcanic terrains in Mexico are different from the ones across Washington state. The WA DNR SLPSTAB is as a western Washington State calibrated hillslope convergence-based susceptibility model. By using this adapted method, the final map becomes a susceptibility map, not a hazard map. Since El Estado watershed is used for the first prototype of this method in volcanic areas in Mexico, landslides and landforms are assessed using a heuristic approach that shows a direct relationship between the occurrence of landslides and the causative terrain parameters in each landform. The heuristic analysis uses the WA DNR general geomorphological criteria such as slope gradient and form, lithology, hydrological conditions, and landslide density to define specific landforms at Pico de Orizaba volcano. As a result, these landforms are considered as homogeneous units that can be represented on any of the hillsides of this volcano. The
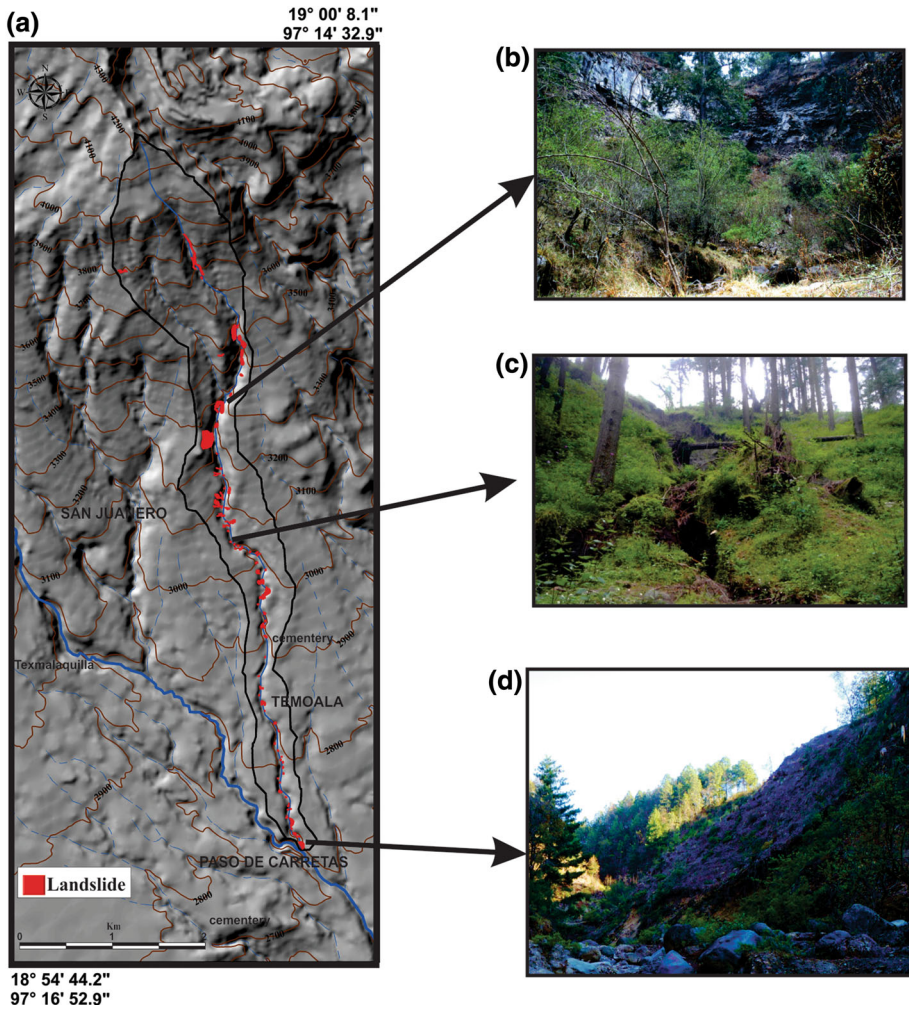
Fig. 2 **a** Landslide inventory (Legorreta et al. 2014), **b** Rockfall deposits in lava flow areas, **c** Shallow landslides and debris flow, **d** Deep-seated landslide

defined landforms in this study are hillslopes with interbeds of pyroclastic flows and lahars (2,690–3,270 m a.s.l.), gravitational deposits (cones and mantles), flat-bottomed valleys (inter-mountain alluvial plain), low-gradient andesitic hillslopes capped with pyroclastic mantles (3,190–3,810 m a.s.l.), steep-gradient dacitic hillslopes covered by pyroclastic falls (3,310–3,990 m a.s.l.), dacitic hillslopes covered by thick pyroclastic falls (4,250–3,960 m a.s.l.), and fluvial valleys. They are more inclusive than the small-scale unstable landforms defined in the Washington landslide hazard protocol, referred to as "rule-identified landforms" (inner gorges, bedrock hollows, convergent headwalls, outer edges of meanders, and active scarps of deep-seated landslides) and non-rule-identified landforms (such as non-rule-identified inner gorges, non-rule-identified bedrock hollow, steep-gradient hillslopes, moderate-gradient hillslopes, and low-gradient hillslopes).

The research begins with collecting background information to provide context, establish a generalized characterization of landslide processes, and define landforms within the

watershed; this involves derivation of a digital elevation model (resolution 3-m) from a topographic map of the area at a scale of 1:20,000 (Instituto Nacional de Estadística y Geografía (INEGI) 2000). Six data layers were obtained from the elevation data: shaded relief, slope angles, slope curvature, contributing area, flow direction, and saturation. Analogue lithological map at a scale of 1:35,000 (Carrasco et al. 1994) is incorporated in the GIS by digitalization of lithological units. The background information also includes a historic landslide inventory map (Fig. 2a) (Legorreta et al. 2014) that is created by identifying and mapping landslide topographic expression—as interpreted from topographic maps—two sets of aerial orthophotographs, thematic layers, and fieldwork. Landslides are mapped and classified into shallow landslides, debris flows, debris slides, deep-seated landslides, earthflows, and rockfalls according to the Landslide Hazard Zonation Protocol (2006) of WA DNR Forest Practices Division, Cruden and Varnes (1996), and Wieczorek (1984). The landslide inventory also has a spatial geo-database of landslide attributes. One of these attributes—landslide parts—allows researchers to separate each mapped landslide into its head scarp, evacuation zone, and deposit (Fig. 3). For the landslide susceptibility zonation analysis, only definitive landslide head scarps are considered. The two sets of orthophotographs that cover a period from 1994 at a scale of 1:20,000–2008 at a scale of 1:10,000 in conjunction with the 3-m resolution DEM and other GIS thematic layers in the GIS and field reconnaissance are used to map landforms. These landforms are identified from primary driving forces of mass wasting based on physical attributes of the landscape such as landslide density, slope gradient, elevation, hydrological characteristics, lithology, and slope convergence.

A preliminary landform product is generated and amended as necessary based on the information from the landslide inventory and aerial photographs. The researcher first identifies stable areas of the landscape, then delineates high-susceptibility landforms. For map legibility, landforms are not smaller than 0.2 hectare (minimum mapping polygon size). Pertinent attributes of mapped landforms are recorded on the GIS geo-dataset. These are: (1) landform identification tag, (2) mass-wasting processes, (3) degree of certainty of the observation, (4) landform area, (5) average landform gradient measured from the 3-m resolution DEM, (6) land use, (7) date of landslide identification on field or on aerial photo, (8) field or aerial photograph identification number, and (9) researcher's comments. Seven landforms derived from physical attributes of the landscape are mapped (Fig. 3). For each landform, semi-quantitative susceptibility ratings are derived from values that correspond to the total area of landslides and the number of landslides within each landform; and they are normalized for the total period of time spanned between the two sets of aerial orthophotographs. These normalized variables are referred to as the landslide area rate (LAR) and the landslide frequency rate (LFR), respectively. Because the resulting numbers are always very small fractions, the values are then multiplied by one million and rounded in order to provide whole easily usable numbers (Washington State Department of Natural Resources, DNR, Forest Practices Division 2006). Using these semi-quantitative calculations, the landslide area rate and landslide frequency rate are entered into a matrix to determine the overall susceptibility rating for each landform. As a result, each landform is assigned a susceptibility rating of Low, Moderate, High, or Very High. Figure 4 shows the procedure for rating each landform.

5 Results

During the assessment of El Estado watershed, a representative sample of 107 mass-wasting features is inventoried, and seven landforms are described in which these mass-
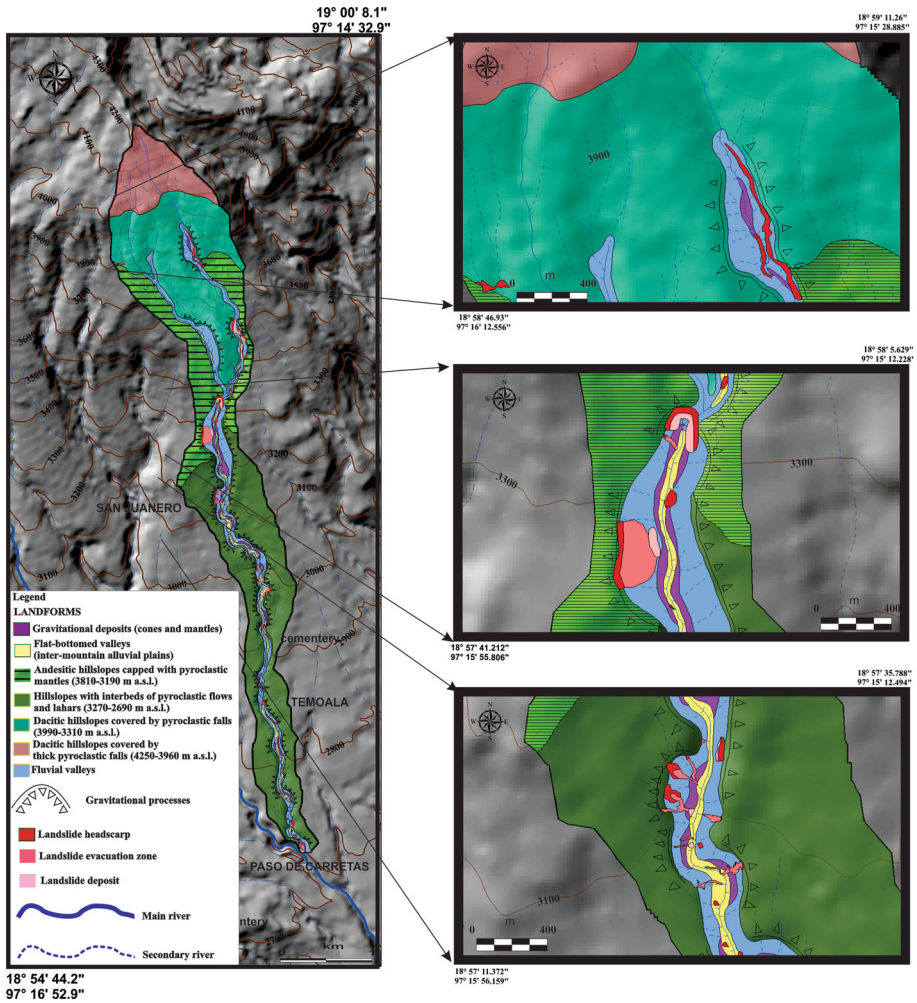
Fig. 3 Landforms and landslide distribution in the El Estado watershed

wasting features are identified. In the study area, shallow undifferentiated failures, debris slides, and debris flows are numerically the predominant landslide types (cumulatively 78.5 %) followed by rockfalls (13.1 %), and deep-seated landslides (8.4 %). Almost three-quarters (73 %) of the mapped landslides are along the fluvial valleys which cover only 11.2 % of the study area. In this landform, debris slide (30.8 %), debris flow (20.6 %), and rockfall (9.3 %) are the predominant landslide types, followed by deep-seated landslides (6.5 %) and shallow landslides (5.6 %). The landform is more prone to landslides in the middle and lower portions of the watershed where there are steep slopes, loose volcanic ash, pyroclastic flow deposits, and volcaniclastic sediments (Fig. 5). Ninety-three percent of all landslides in this landform are at elevations between 2,677 and 3,640 m a.s.l. The remaining landslides are in landforms with weathered, massive, blocky, or brecciated andesitic and dacitic lava flows and lahars covered by fall deposits (Table 1).

The landforms predict areas that pose susceptibility for mass wasting (Fig. 5) and are as follows:
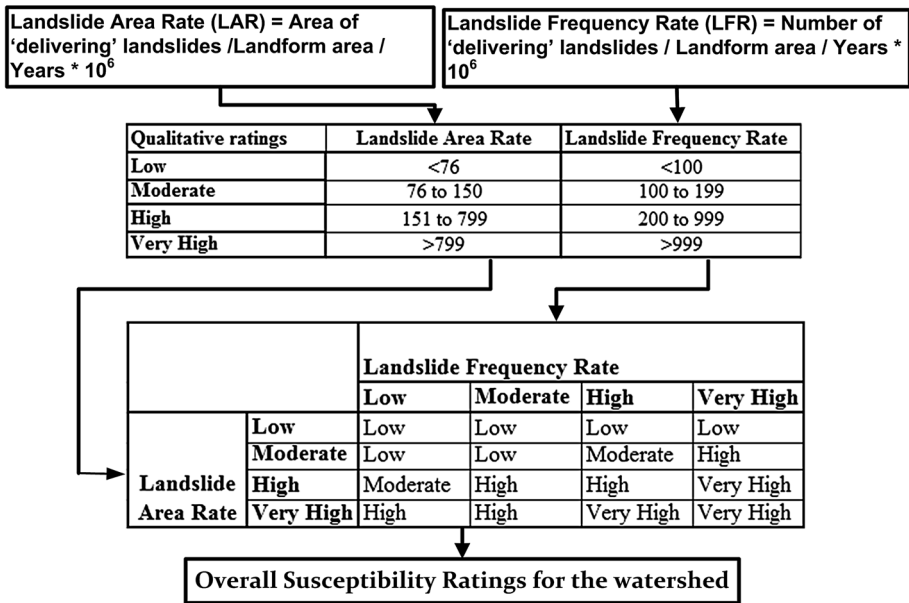
Landslide Area Rate (LAR) = Area of 'delivering' landslides /Landform area / Years * 10^6

Landslide Frequency Rate (LFR) = Number of 'delivering' landslides / Landform area / Years * 10^6

Qualitative ratings	Landslide Area Rate	Landslide Frequency Rate
Low	<76	<100
Moderate	76 to 150	100 to 199
High	151 to 799	200 to 999
Very High	>799	>999

		Landslide Frequency Rate			
		Low	Moderate	High	Very High
	Low	Low	Low	Low	Low
	Moderate	Low	Low	Moderate	High
Landslide	High	Moderate	High	High	Very High
Area Rate	Very High	High	High	Very High	Very High

Overall Susceptibility Ratings for the watershed

Fig. 4 General procedure for producing a semi-quantitative overall susceptibility rating per landform

(1) Gravitational deposits (cones and mantles) cover 1.44 % of the watershed area and contain 12.15 % of the mapped landslides. Their potential for mass wasting and delivery is very high. These areas may occur intermittently in lateral extent along the fluvial valleys and include all slope forms (convergent, divergent, and planar) that range between 0 and 53 %. In some places where lava flow walls are present, the values exceed 100 % (>45°). This category is contained in other high-susceptibility landforms (fluvial valleys). The gravitational deposits are the initiation points for many debris slides and shallow landslides.

(2) Flat-bottomed valleys (inter-mountain alluvial plains) cover 2.84 % of the area and contain 1.87 % of the mapped landslides. Their potential for mass wasting and delivery is high. The average slope on flat-bottom valleys is 36 %. Although the landform includes slope forms that are mostly gentler than 10 %, it is possible to find cuts with slopes >100 %. This category consists predominantly of lowland forms such as valley bottoms, floodplains, and flat terrace surfaces. Shallow landslides occur through stream undercutting of the outer edges of valley walls or high terraces of an unconfined meandering stream.

(3) Andesitic hillslopes capped with pyroclastic mantles (3,810–3,190 m a.s.l.) cover 14.96 % of the area, contain 2.8 % of the mapped slope failures, and include all slope forms (convergent, divergent, and planar). They include slope forms that have gradients of <10 %, but on average the gradient is higher than 37 %. The potential for mass wasting and delivery is high. Rock topples and falls and debris slides can occur along the channel where lava flows form steep steps.

(4) Hillslopes with interbeds of pyroclastic flows and lahars (3,270–2,690 m a.s.l.) cover 34.14 % of the area, contain 8.41 % of the mapped slope failures, and include all slope forms (convergent, divergent, and planar). They include slope forms that
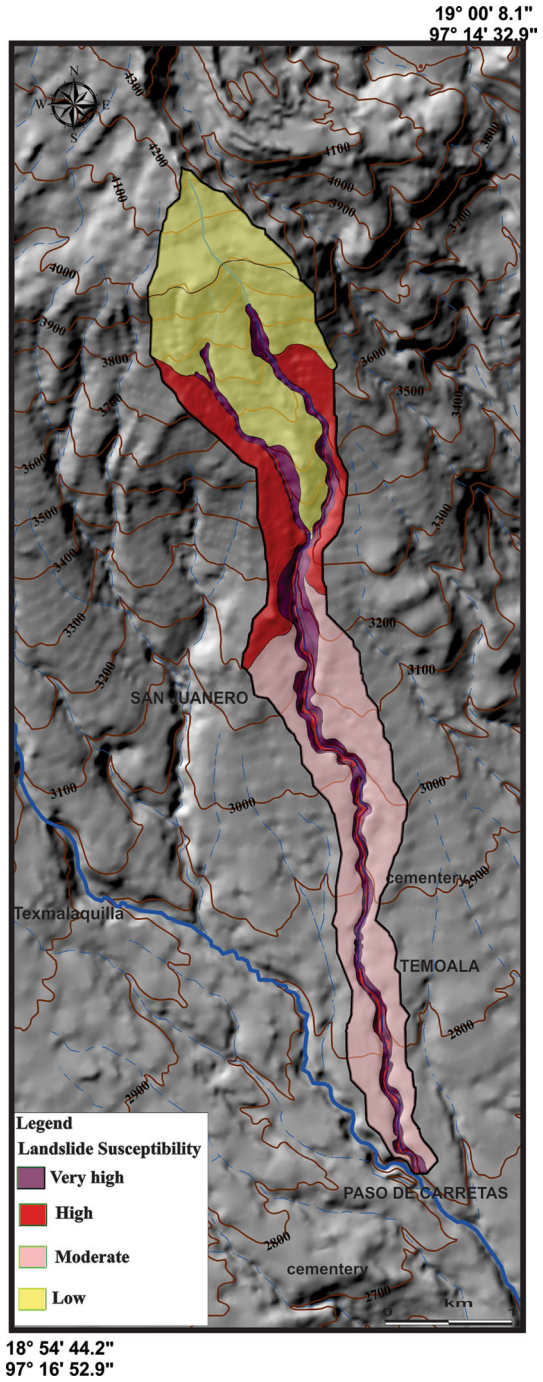
Fig. 5 Landslide susceptibility
map

Table 1 Landslides mapped in the El Estado watershed

Landform	Landslide type						Total
	Shallow landslides	Debris flows	Debris avalanches/slides	Deep-seated landslides	Earthflows	Rock topples and falls	
Gravitational deposits (cones and mantles)	1	0	9	1	0	2	13
Flat-bottomed valleys (inter-mountain alluvial plains)	1	0	0	1	0	0	2
Low-gradient andesitic hillslopes capped with pyroclastic mantles (3,810–3,190 m a.s.l.)	0	1	0	0	0	2	3
Hillslopes with interbeds of pyroclastic flows and lahars (3,270–2,690 m a.s.l.)	1	7	1	0	0	0	9
Steep-gradient dacitic hillslopes covered by pyroclastic falls (3,990–3,310 m a.s.l.)	2	0	0	0	0	0	2
Dacitic hillslopes covered by thick pyroclastic falls (4,250–3,960 m a.s.l.)	0	0	0	0	0	0	0
Fluvial valleys	6	22	33	7	0	10	78
Total	11	30	43	9	0	14	107

are mostly on average <23 %. This category contains other high-susceptibility landforms (fluvial valleys) that are the initiation points for many shallow landslides, debris slides, and debris flows. In the boundary areas with high-susceptibility landforms, the gradient is higher than 100 %. Their potential for mass wasting and delivery is moderate.

(5) Dacitic hillslopes covered by pyroclastic falls (3,990–3,310 m a.s.l.) cover 24.82 % of the area and contain 1.87 % of the mapped slope failures. The landform forms a pyroclastic ramp that includes all slope forms (convergent, divergent, and planar) and average gradients of >47 %. The potential for mass wasting and delivery is low. This category contains fluvial valleys that are the initiation points for many shallow landslides, rockfalls, debris slides, and debris flows.

(6) Dacitic hillslopes covered by thick pyroclastic falls (4,250–3,960 m a.s.l.) cover 10.57 % of the area. No landslide is mapped. This category represents areas whose surface expression is characterized by flat to slightly undulating and uneven hills with little dissection and slopes averaging 27.85 %. The potential for mass wasting and delivery is low.

(7) Fluvial valleys cover 11.23 % of the watershed area and contain 72.9 % of the mapped landslides. Their potential for mass wasting and delivery is very high. Asymmetrical and symmetrical fluvial valleys occur intermittently in lateral extent. Slopes are generally >70 %, although these gorge systems may fail on convergence with planar slopes of <65 %.

6 Conclusions

In this paper, we briefly introduce and review the implementation of a method for determining landslide susceptibility per landform in volcanic terrain. The method is implemented by adapting the WA DNR Forest Practices Landslide Hazard Zonation Protocol for the standardization and integration of thematic layers, dividing the landscape into geomorphically distinct landform areas; and it entails a landslide susceptibility calculation for each landform instead of a landslide hazard calculation. The final map from the adapted landslide hazard method is a susceptibility map, because the method does not incorporate the analysis of the probability of landslide occurrence within a specified period of time by using the WA DNR SLPSTAB susceptibility model (Bilderback and Brunengo 2007; Shaw and Johnson 1995). Implementing and developing a GIS-based landslide susceptibility zonation method in conjunction with the landslide inventory map and its related geodatabase gives a fundamental piece of information for land managers and researchers.

In this study, the susceptibility map (Fig. 5) shows that dacitic hillslopes in the upper portion of the watershed are less susceptible to landslides. In these landforms, lava flows below the pyroclastic deposit act as sponges to hold the surface water and occasionally produce rockfalls. In the middle portion of the watershed where lahar deposits are capped with pyroclastic deposits, the susceptibility is high and shallow, and deep-seated landslides are the predominant process. The steep slopes in the valleys where lava flows occasionally produce rockfalls and where the land use disrupts the strength of soil to produce deep-seated and shallow landslides are rated with high and very high susceptibility. This finding is important because the landform has a small forest buffer between 50 and 100 m. This small buffer is the result of decades of deforestation and modification of the slopes in favor of agricultural activities. The small buffer of vegetation around the valleys is unable to stop

the disruption of the slope, allowing the geological conditions in conjunction with anthropogenic land use changes to trigger an abundance of landslides and landslide sediment production. The coalescence of the up-stream landslide sediments in the watershed increases the destructive power of debris flows that threaten towns such as Córdova, Orizaba, Río Blanco, Nogales, and Ciudad Mendoza, with a total population of 360,000 people. Thus, this buffer area in the landform needs preventive and corrective measures.

The study at Rio El Estado is an attempt to produce the prototype of a standardized methodology for future landslide susceptibility and hazard maps of volcanic regions in Mexico. This adaptation of the Washington Landslide Hazard Zonation Protocol is subject to modification and improvement with further assessment and comparison with other watersheds at Pico de Orizaba and perhaps in other volcanic regions. The researchers acknowledge the technical limitation of the landslide susceptibility map obtained by using a landslide hazard method as well as the landform map, whose quality depends on the experience of the investigators, the goals of the project, the complexity of the study area, the landslide inventory, and the available information. For instance, as a first prototype defining and delimiting specific volcanic landforms is based on geomorphological experience that allows researchers to create a framework for future identification of geomorphological units in other volcanic watersheds. The limitations of subjectivity and reproducibility of this heuristic approach can be reduced by following morphometric parameters and procedures or by automatic geomorphological mapping and statistical analysis.

Despite the limitations, the authors see the landform map and the landslide susceptibility calculations of El Estado watershed as a method with potential to be the foundation of an integrated means to handle and support prognostic studies of slope instability. For example, the semi-quantitative rating for homogeneous volcanic landforms will provide the basis for landslide hazard/susceptibility comparison among other volcanic watersheds.

Future research should:

(1) Create a hazard map by incorporating the analysis of a multiple logistic regression (MLR) susceptibility model (Legorreta et al. 2014) to produce the landslide hazard zonation map.
(2) Calibrate the model with other watersheds at different cartographic scales, DEM resolutions, and sampling strategies to make the model more statistically reliable and standardized.
(3) Assess and model landslide hazard and the sediment production of individual landslide types.
(4) Make the maps and analysis available to the public via web download as soon as they are created and approved.

References

Anbalagan R, Bhawani S (1996) Landslide hazard and risk assessment mapping of mountainous terrains- a case study from Kumaun Himalaya, India. Eng Geol 43:237–246

Bilderback EL, Brunengo MJ (2007) Landslide hazard zonation project—Skamokawa watershed, Wahkiakum County, Washington. Washington department of natural resources. http://www.dnr.wa.gov/BusinessPermits/Topics/LandslideHazardZonation/Pages/fp_lhz_completed.aspx

Blahut J, Sterlacchini S, Van Westen CJ (2010) Analysis of landslide inventories for accurate prediction of debris-flow source areas. Geomorphology 119(1–2):36–51

Bocco VG (1983) La zonalidad geomorfológica de la región comprendida en la carta Querétaro: 1:250,000. En: Memoria del IX Congreso Nacional de Geografía. Tomo I, México, pp 28–36

Bolongaro-Crevenna A, Torres-Rodríguez V, Sorani V, Frame D, Ortiz MA (2005) Geomorphometric analysis for characterizing landforms in Morelos state, Mexico. Geomorphology 67:407–422

Borga M, Fontana GD, Cazorzi F (2002) Analysis of topographic and climatic control on rainfall-triggered shallow landsliding using a quasi-dynamic wetness index. J Hydrol 268:56–71

Capra L, Lugo-Hubp J (2006) Fenómenos de remoción en masa en el poblado de Zapotitlán de Méndez, Puebla: relación entre litología y tipo de movimiento. Rev Mex de Cienc Geol 20(2):95–106

Carrasco-Núñez G, Ban M (1994) Geologic map and structure sections of the summit area of Citlaltepetl Volcano, Mexico, with summary of the geology of the Citlaltépetl volcano summit area. Cartas geológicas y mineras. Institute of Geology, UNAM, p 9

Centro Nacional de Prevención de Desastres (2001) Las cenizas volcánicas del Popocatépetl y sus efectos para la aeronavegación e infraestructura aeroportuaria. Instituto de Geofísica, UNAM

Chinnayakanahalli K, Tarboton DG, Pack RT (2003) An objective method for the intercomparison of terrain stability models. Eos Trans Am Geophys Union 84(46):H31C–0480

Corominas J, Moya J (2008) A review of assessing landslide frequency for hazard zoning purposes. Eng Geol 102:193–213

Cruden M, Varnes D (1996) Landslide types and processes. In: Turner AK, Shuster RL (eds) Landslides: investigation and mitigation. Transportation Research Board, Special Report, 247, p 36–75

De la Cruz-Reyna S, Carrasco-Núñez G (2002) Probabilistic hazard analysis of Citlaltépetl (Pico de Orizaba) Volcano, eastern Mexican Volcanic Belt. J Volcanol Geotherm Res 113:307–318

Dietrich WE, Bellugi DG, Sklar LS, Stock JD, Heimsath AM, Roering JJ (2003) Geomorphic transport laws for predicting landscape form and dynamics. In: Wilcock PR, Iverson RM (eds) Prediction in geomorphology. Geophysical monograph, 135. American Geophysical Union, Washington DC, pp 103–132

Dikau R, Brabb EE, Mark RK, Pike RJ (1995) Morphometric landform analysis of New Mexico. Z Fur Geomorphol 101:109–126

Evans IS (2012) Geomorphometry and landform mapping: what is a landform? Geomorphology 137(1):94–106

Guzzetti F, Carrara A, Cardinali M, Reichenbach P (1999) Landslide hazard evaluation: a review of current techniques and their application in a multi-scale study, central Italy. Geomorphology 31:181–216

Hammond C, Hall D, Miller S, Swetik P (1992) Level I stability analysis (LISA) documentation for version 2.0. General technical report INT-285, US Department of Agriculture, Forest Service, Intermountain Research Station, Ogden, UT, 190

Haneberg WC (2005) New quantitative landslide hazard assessment tools for planners. In: Schwab JC, Gori PL, Jeer S (eds) Landslide hazards and planning, planning advisory service report number 533/534. American Planning Association, Chicago, pp 76–84

Hervás J, Bobrowsky P (2009) Mapping: inventories, susceptibility, hazard and risk. In: Sassa K, Canuti P (eds) Landslides—disaster risk reduction. Springer, Berlin, pp 321–349. ISBN 978-3-540-69966-8

Hubbard BE (2001) Volcanic hazard mapping using aircraft, satellite and digital topographic data: Pico de Orizaba (Citlaltépetl), México. Thesis. Department of Geology, State University of New York

Hubbard BE, Sheridan MF, Carrasco-Nunez G, Díaz-Castellon R, Rodriguez S (2007) Comparative lahar hazard mapping at Volcan Citlaltépetl, Mexico using SRTM, ASTER and DTED-1 digital topography. J Volcanol Geotherm Res 160(1):99–124

Instituto Nacional de Estadística y Geografía (2000) Carta topográfica La Perla, Veracruz de Ignacio de la Llave E14B56A. Escala 1:20,000. http://www.inegi.org.mx/geo/contenidos/topografia/carta1_20000.aspx

Instituto Nacional de Estadística y Geografía (2010) Censo de población y vivienda 2010. http://www.inegi.org.mx/Sistemas/temasV2/Default.aspx?s=est&c=17484

Iwahashi J, Pike R (2007) Automated classifications of topography from DEMs by an unsupervised nested-means algorithm and a three-part geometric signature. Geomorphology 86:409–440

Iwahashi J, Watanabe S, Furuya T (2001) Landform analysis of slope movements using DEM in Higashikubiki area, Japan. Comput Geosci 27(7):851–865

Jasiewicz J, Stepinski T (2013) Geomorphons—a pattern recognition approach to classification and mapping landforms. Geomorphology 182:147–156

Lee S, Ryu JH, Won JS, Park HJ (2004) Determination and application of the weights for landslide susceptibility mapping using an artificial neural network. Eng Geol 71:289–302

Legorreta PG, Bursik M (2009) Assessment of landslides susceptibility: LOGISNET: a tool for multi-method, multilayer slope stability analysis. ISBN 9783639154771. VDM Verlag Dr. Muller, USA. 360

Legorreta PG, Serdar C, Goetz V (2008) An overview of the Washington State Department of Natural Resources, Forest Practices Division's landslide hazard zonation project methodology and products for identification of unstable slopes. Paper 148312. Proceedings from the 5–9 Oct 2008 Geological Society of America Joint Meeting, Houston, TX

Legorreta PG, Bursik M, Lugo HJ, Paredes-Mejía LM, Aceves-Quesada JF (2014) A GIS method for landslide inventory and susceptibility mapping in the Río El Estado watershed, Pico de Orizaba volcano Mexico. Nat Hazards J. 71(1):229–241. doi:10.1007/s11069-013-0911-8

Minar J, Evans I (2008) Elementary forms for land surface segmentation: the theoretical basis of terrain analysis and geomorphological mapping. Geomorphology 95:236–259

Montgomery DR, Dietrich WE (1994) A physical based model for the topographic control on shallow landslides. Water Resour Res 30:1153–1171

Morrissey MM, Wieczorek GF, Morgan BA (2001) A comparative analysis of hazard models for predicting debris flows in Madison County, Virginia. US Geological Survey Open-File Report 01-0067, 17. http://pubs.usgs.gov/of/2001/ofr-01-0067/ofr-01-0067.htmls

Pack RT, Tarboton DG, Goodwin CN (1998) The SINMAP approach to terrain stability mapping. Originally cited in: Proceedings of the Eighth Congress of the International Association of Engineering Geology. Vancouver, British Columbia, Canada. Retrieved from http://hydrology.neng.usu.edu/sinmap/

Parise M (2001) Landslide mapping techniques and their use in the assessment of the landslide hazard. Phys Chem Earth Part C 26(9):697–703

Pennock D, Zebarth B, De Jong E (1987) Landform classification and soil distribution in hummocky terrain, Saskatchewan, Canada. Geoderma 40:297–315

Pérez-Gutiérrez R (2007) Análisis de la vulnerabilidad por los deslizamientos en masa, caso: Tlacuitlapa, Guerrero. Bol de la Soc Geol Mex 59(2):171–181

Pike RJ, Dikau R (1995) Advances in geomorphometry. Z fur Geomorphol 101:238

Qiu C, Esaki T, Xie M, Mitani Y, Wang C (2006) A GIS system development for evaluating 3d slope stability. ESRI. Retrieved 1 Jan 2006 from http://gis.esri.com/library/userconf/proc05/abstracts/a1158.html

Secretaría de Protección Civil (2010) Atlas de peligros geológicos e hidrometeorológicos del estado de Veracruz. In: Gonzalez IM, Barrera WM, Elizarraras SR, Xalapa (eds) Secretaría de Protección Civil del estado de Veracruz. Universidad Veracruzana, UNAM

SEDESOL (2011) Atlas de Riesgos (o peligros) naturales del municipio de Nogales, Veracruz 2011. Municipio de Nogales, Veracruz 58

Shaw SC, Johnson DA (1995) Slope morphology model derived from digital elevation data. Proceedings for the 23–25 Oct 1995 Northwest Arc/Info Users Conference, Coeur d'Alene, Idaho, 13

Sheridan MF, Carrasco-Nuñez G, Hubbard BE, Siebe C, Rodriguez-Elizarraraz S (2001) Mapa de peligros del Volcan Citlaltépetl (Pico de Orizaba) 1:250,000 scale. Universidad Nacional, Autonoma Mexico, Institute of Geography

Stallins JA (2006) Geomorphology and ecology: unifying themes for complex systems in biogeomorphology. Geomorphology 77:207–216

Tapia-Varela G, López-Blanco J (2002) Mapeo geomorfológico analítico de la porción central de la Cuenca de México a escala 1.100,000. Rev. Mexicana de Ciencias Geológicas, UNAM, 19(1):50–65

Van Westen CJ, Rengers N, Terlien MTJ, Soeters R (1997) Prediction of the occurrence of slope instability phenomena through GIS-based hazard zonation. Geol Rundsch 86(2):404–414

Vaugeois LM (2003) An overview of the Washington State Department of Natural Resources, Forest Practices division's landslide hazard zonation project methodology and products for identification of unstable slopes. (Abstract). Proceedings from the November 2–5 Geological Society of America Annual Meeting in Seattle, WA. 35(6):432

Verma SP (1987) Mexican Volcanic Belt: present state of knowledge and unsolved problems. Geofísica Internacional 26:309–340

Washington State Department of Natural Resources, DNR, Forest Practices Division. (2006). Landslide hazard zonation mapping protocol version 2.0 retrieved from: http://www.dnr.wa.gov/BusinessPermits/Topics/LandslideHazardZonation/Pages/fp_lhz_review.aspx

Wieczorek GF (1984) Preparing a detailed landslide inventory map for hazard evaluation and reduction. Bull As Eng Geol 21:337–342

Xie M, Esaki T, Qiu C, Wang C (2006) Geographical information system-based computational imple-
    mentation and application of spatial three-dimensional slope stability analysis. Comput Geosci
    33(4–5):260–274
Zhou G, Esaki T, Mitani Y, Xie M, Mori J (2003) Spatial probabilistic modeling of slope failure using an
    integrated GIS Monte Carlo simulation approach. Eng Geol 68:373–386
Zinck JA (2013) Geopedology: elements of geomorphology for soil and geohazard studies. ITC, Enschede,
    p 127. ISBN 978-90-6164-352-4